Polarization anisotropic transmission through metallic Sierpinski-Carpet aperture array

Yuan Chen, Li Zhan,* Jian Wu, and Tianmeng Wang

Department of Physics, Key Laboratory for Laser Plasmas (Ministry of Education), State Key Lab of Advanced Optical Communication Systems and Networks, Shanghai Jiao Tong University, Shanghai 200240, China
lizhan@sjtu.edu.cn

Abstract: Extraordinary optical transmission through rectangular Sierpinski -Carpet aperture array on an Ag film has been observed. Attributed to the fractal-featured rectangle array, it exhibits polarization dependence and dual-band transmission simultaneously. In addition, the incident angle invariance transmission displays within a certain angle range, which is quite different from ordinary rectangles. This report provides a way to achieve the polarization-manipulated multi-band transmission in infrared region.

OCIS codes: (240.0310) Thin films; (240.6680) Surface plasmons; (240.6690) Surface waves; (240.0240) Optics at surfaces.

References and links

1. H. A. Bethe, "Theory of diffraction by small holes," Phys. Rev. **66**(7-8), 163–182 (1944).
2. T. W. Ebbesen, H. J. Lezec, H. F. Ghaemi, T. Thio, and P. A. Wolff, "Extraordinary optical transmission through sub-wavelength hole arrays," Nature **391**(6668), 667–669 (1998).
3. K. J. Koerkamp, S. Enoch, F. B. Segerink, N. F. van Hulst, and L. Kuipers, "Strong influence of hole shape on extraordinary transmission through periodic arrays of subwavelength holes," Phys. Rev. Lett. **92**(18), 183901 (2004).
4. Y. Qiu, L. Zhan, and Y. Xia, "Polarization-manipulated dual-band enhanced optical transmission through sub-wavelength rectangular hole array on metallic film," IEEE J. Sel. Top. Quantum Electron. **19**(3), 4600106 (2013).
5. K. L. van der Molen, K. Koerkamp, S. Enoch, F. B. Segerink, N. F. van Hulst, and L. Kuipers, "Role of shape and localized resonances in extraordinary transmission through periodic arrays of subwavelength holes: Experiment and theory," Phys. Rev. B **72**(4), 045421 (2005).
6. D. E. Grupp, H. J. Lezec, T. W. Ebbesen, K. M. Pellerin, and T. Thio, "Crucial role of metal surface in enhanced transmission through subwavelength apertures," Appl. Phys. Lett. **77**(11), 1569–1571 (2000).
7. E. Popov, M. Neviere, S. Enoch, and R. Reinisch, "Theory of light transmission through subwavelength periodic hole arrays," Phys. Rev. B **62**(23), 16100–16108 (2000).
8. J. H. Kim and P. J. Moyer, "Transmission characteristics of metallic equilateral triangular nanohole arrays," Appl. Phys. Lett. **89**(12), 121106 (2006).
9. E. C. Kinzel and X. F. Xu, "Extraordinary infrared transmission through a periodic bowtie aperture array," Opt. Lett. **35**(7), 992–994 (2010).
10. K. L. van der Molen, F. B. Segerink, N. F. van Hulst, and L. Kuipers, "Influence of hole size on the extraordinary transmission through subwavelength hole arrays," Appl. Phys. Lett. **85**(19), 4316–4318 (2004).
11. W. J. Wen, Z. Yang, G. Xu, Y. H. Chen, L. Zhou, W. K. Ge, C. T. Chan, and P. Sheng, "Infrared passbands from fractal slit patterns on a metal plate," Appl. Phys. Lett. **83**(11), 2106–2108 (2003).
12. W. Wen, L. Zhou, B. Hou, C. Chan, and P. Sheng, "Resonant transmission of microwaves through subwavelength fractal slits in a metallic plate," Phys. Rev. B **72**(15), 153406 (2005).
13. Y. Qiu, X. Hu, L. Zhan, Q. Shen, and Y. Xia, "Near-infrared polarization-manipulated anisotropic transmission through metallic array of subwavelength fractal slits," IEEE Photon. Technol. Lett. **23**(10), 630–632 (2011).
14. A. Degiron and T. Ebbesen, "The role of localized surface plasmon modes in the enhanced transmission of periodic subwavelength apertures," J. Opt. A, Pure Appl. Opt. **7**(2), S90–S96 (2005).
15. Y.-W. Jiang, L. D. Tzuang, Y.-H. Ye, Y.-T. Wu, M.-W. Tsai, C.-Y. Chen, and S.-C. Lee, "Effect of Wood's anomalies on the profile of extraordinary transmission spectra through metal periodic arrays of rectangular subwavelength holes with different aspect ratio," Opt. Express **17**(4), 2631–2637 (2009).
16. M. A. Ordal, L. L. Long, R. J. Bell, S. E. Bell, R. R. Bell, R. W. Alexander, Jr., and C. A. Ward, "Optical properties of the metals al, co, cu, au, fe, pb, ni, pd, pt, ag, ti, and w in the infrared and far infrared," Appl. Opt. **22**(7), 1099–1119 (1983).
17. A. Degiron, H. Lezec, N. Yamamoto, and T. Ebbesen, "Optical transmission properties of a single subwavelength aperture in a real metal," Opt. Commun. **239**(1-3), 61–66 (2004).

#202368 - $15.00 USD Received 2 Dec 2013; revised 17 Jan 2014; accepted 17 Jan 2014; published 27 Jan 2014

18. Z. Ruan and M. Qiu, "Enhanced transmission through periodic arrays of subwavelength holes: the role of localized waveguide resonances," Phys. Rev. Lett. **96**(23), 233901 (2006).
19. C. Genet and T. W. Ebbesen, "Light in tiny holes," Nature **445**(7123), 39–46 (2007).
20. Y. Qiu, L. Zhan, X. Hu, S. Luo, and Y. Xia, "Demonstration of color filters for OLED display based on extra-ordinary optical transmission through periodic hole array on metallic film," Displays **32**(5), 308–312 (2011).

1. Introduction

According to the classical diffraction theory, when light illuminates on an infinitely thin perfect conductor with a hole on it, the transmission is proportional to $(r/\lambda)^4$ (r is the radius of the hole and λ is the wavelength of incident light) [1]. Generally, the transmission is very low when λ is much larger than r. However the experiment reported by Ebbesen *et al* has proved that this prediction is not absolute [2]. They showed that the transmission by area normalization in periodic subwavelength hole arrays is over 2 at the maxima, which is the well known extraordinary optical transmission (EOT). In order to explore the mechanism of this phenomenon, various factors, including the type of metal, film depth, hole shape and the period have been investigated respectively [3–5]. Thanks to the development of the micro fabrication technology, fine structure processing on metallic films becomes available. Many different patterns were manufactured and studied, such as ellipses, rectangles, squares, triangles and even bowties [6–9]. According to the previous reports, it is not hard to conclude that the hole shape plays an important role on the transmission spectrum [3, 5, 10]. Recently, the fractal-featured structures have attracted much attention due to their good self-similarity and excellent compressibility. For instance, in the 'I-shaped' fractal-featured subwavelength structure, it exhibits strong frequency selective transmission and excellent incident invariance transmission. The shape effect caused by localized surface plasmons (LSPs) plays an important part in their distinct properties [11–13]. However, each hole element in these structures is a self-similar geometry, but the whole structure of the array is not.

The rectangular Sierpinski-Carpet (RSC) aperture array studied in this paper is an overall self-similar structure, which is constructed by many different size ordinary rectangles. This is quite different from the structure mentioned above. Here, a RSC is composed of different sized rectangles, and a part in it is similar to the single RSC. The transmission spectra for various polarized states and incidence angles have been studied both in the simulations and experiments. It is found that, the x- and y-axis polarized incidence permeates different wavelengths respectively, but the transmission peaks almost do not change when the incident angle varies. The former is in accord with the property of the rectangular hole array while the latter is not [14, 15]. This distinct property stems from the influence of the tiny spacing between the small holes and the big ones, which affects both the surface plasmon polaritons (SPPs) and the localized surface plasmons (LSPs). This structure achieves the polarization-manipulated anisotropic transmission and incident angle invariance.

2. Experimental structure and theory

The structure shown in Fig. 1 is constructed in the following way. A rectangle is cut into 9 congruent sub-rectangles in a 3-by-3 grid, and the central sub-rectangle is removed. The same procedure is then applied to the remaining 8 sub-rectangles. In the structure, there are three size rectangles: the smallest one 'A' is 0.1×0.2 μm^2, the medium one 'B' is 0.3×0.6 μm^2 and the biggest one in the center 'C' is 0.9×1.8 μm^2. It is easy to find that the magnified part shown in Fig. 1(b) is similar to the single structure. The simulations in this work were calculated by using the Photonic Software OptiFDTD, and periodic boundary conditions (PBCs) were used in calculation [16].

The sample lies in the x-y plane and the incident light is along z-axis as shown in Fig. 1(c). The calculated zero-order transmission spectra of the single RSC fractal pattern at different polarization angles are shown in Fig. 2. There are two main peaks when the light is x-axis polarized and incident perpendicularly. One locates at 788 nm and the other is at ~1.97 μm. The wide peak spacing makes it easy to distinguish them. The transmission rate is about 0.7. There are two sets of transmission peaks along y-axis polarization. One set is at 755 nm

#202368 - $15.00 USD Received 2 Dec 2013; revised 17 Jan 2014; accepted 17 Jan 2014; published 27 Jan 2014

and 930 nm, and another is at 1.88 μm and 2.16 μm. According to these results, this structure exhibits polarization-dependence transmission.

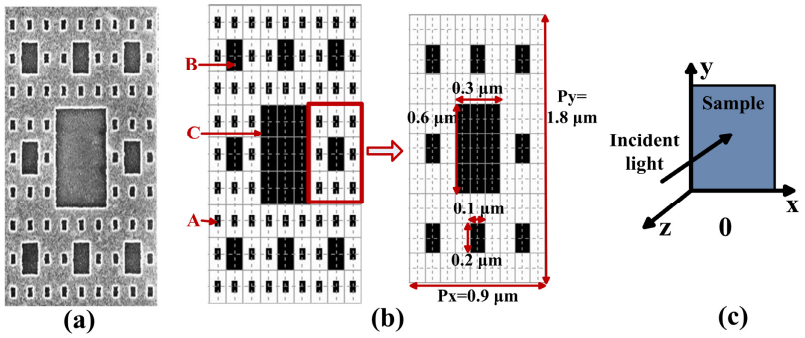

Fig. 1. (a) The SEM image of the single structure on the Ag film. (b) The simulated single structure on the Ag film (left panel) and the magnified part (right panel) as a single element. The single structure is 2.7 × 5.4 μm^2. The specific parameters of the single element are shown in right panel. The period along x-axis P_x is 0.9 μm and along y-axis P_y is 1.8 μm. (c) The sketch of incident light direction.

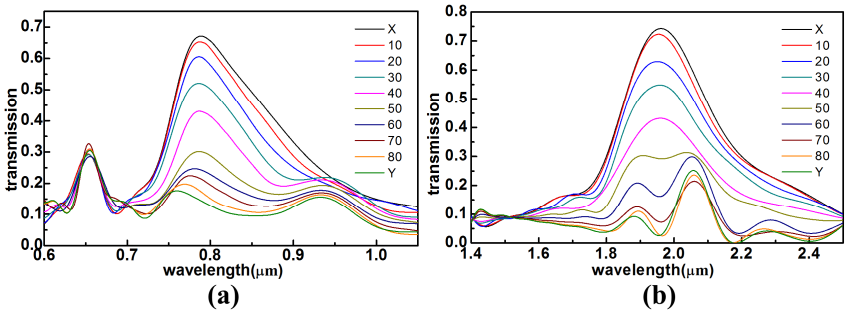

Fig. 2. The transmission spectra of different polarization angles. (a) In the short wavelength (SW) region, below 1 μm. (b) In the long wavelength (LW) region, beyond 1 μm.

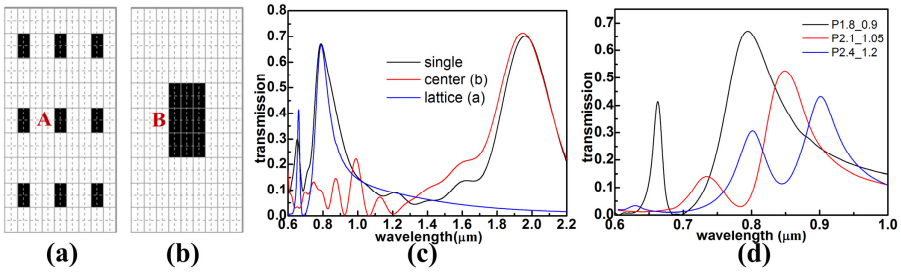

Fig. 3. The divided parts of the single element: (a) the rectangular lattice and (b) the center rectangle. (c) The zero-order transmission of each part. (d) The x-axis polarized spectra of the rectangle array with the same size hole in different periods. The parameters of the lattice: P_x = 0.9 μm, P_y = 1.8 μm (black line); P_x = 1.05 μm, P_y = 2.1 μm (red line); P_x = 1.2 μm, P_y = 2.4 μm (blue line).

The magnified part in Fig. 1(b) is taken as a single element. It is then divided into two components to investigate the effects of the two size rectangles. One is the center big rectangle 'B' and another is a rectangular lattice which consists of nine “A's'. The structures and the calculated transmissions in x-axis polarization are shown in Fig. 3. It is well demonstrated that the short wavelength (SW) peak is dominated by the small apertures, and the long wavelength (LW) one is mainly affected by the center big rectangle. The

#202368 - $15.00 USD Received 2 Dec 2013; revised 17 Jan 2014; accepted 17 Jan 2014; published 27 Jan 2014

transmission spectrum of the RSC structure is a superposition of the effect of the center rectangle and that of the lattice. For array structure, the transmission is primarily due to SPPs. Then the transmission spectra in different periods are calculated to clarify the SPP effects. For comparison, the period along x-axis P_x is changed to 1.05 μm and 1.2 μm, and the period along y-axis P_y to 2.1 μm and 2.4 μm, respectively. But the hole sizes are the same. The transmission spectra in x-axis polarization are shown in Fig. 3(d). It is found that the peak has a red shift as the period increases, which well demonstrates the effect of the period. This indicates that the SPPs play a key role on the transmission.

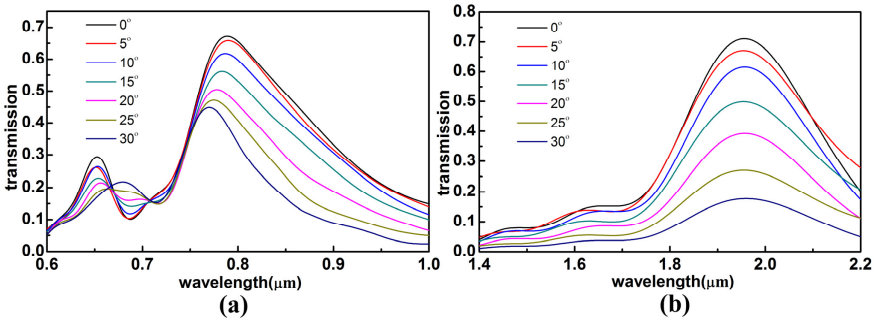

Fig. 4. (a) The transmission of the SW peak and (b) the transmission of the LW peak, under different incident angles with a step change of 5 degrees.

The rectangle has poor oblique invariance because of its asymmetry [17, 18]. However, the results seem to be quite different when many rectangles are constructed together according to some order. Angle invariance transmission was unexpectedly displayed when many slits composed an 'I-shaped' fractal-featured structure [13]. To further investigate whether the proposed structure has the same property, the transmission spectra of different incident angles have been studied. The simulation results in Fig. 4 exhibits that the peaks barely change while the intensities vary obviously. In the SW region, the peak has a blue shift ~20 nm while the intensity decreases 21%, and the one in the LW region is still located at ~1.97 μm with the intensity dramatically decreasing from 71% to 18%. Here, the positions of transmission peaks are almost no change, which is quite different from the rectangular hole arrays [3, 17]. If the transmission is only determined by the periodic array, the peaks are supposed to be changed in oblique incidence according to the momentum matching condition [19]. However, there is no significant shift on the location in the simulation results. There must be some other effects on the transmission. The surface energy flux distributions in Fig. 5 well display the respective role of the two parts of the structure. It is also shown that the tiny distance between the center rectangle and the small ones around affects the localized resonance around the holes, which is responsible for the invariance transmission.

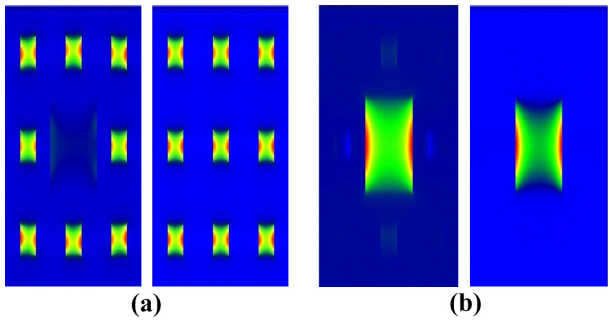

Fig. 5. The surface energy flux distributions of the two peaks in x polarization. (a) At 788 nm, the single element (left panel) and the rectangular lattice (right panel). (b) At 1.97 μm, the single element (left panel) and the center big rectangle (right panel).

#202368 - $15.00 USD Received 2 Dec 2013; revised 17 Jan 2014; accepted 17 Jan 2014; published 27 Jan 2014

3. Results and discussion

The Scanning Electron Microscope (SEM) image of the single structure is shown in Fig. 1(a). A silver film with thickness of 50 nm was deposited on a quartz substrate with a 2 nm Cr buffer layer. Polymethylmethacrylate (PMMA) was then spin coated onto the silver film, followed by electron-beam (Raith 150) exposure to define the pattern regions. After being developed and fixed, the PMMA-patterned silver film was etched using reactive ion etching system (PlasmaLab 80 Plus, Oxford Instruments). Finally by removing the PMMA with acetone, the whole sample was prepared. The total etching area was 162 × 324 μm^2 with 60 periods. Due to the small size of the apertures and the limitation of the etching technique we used, the sample film was just 50 nm thick. All the transmission spectra of the sample were measured by a Vertex 70 FT-IR Spectrometer (Bruker) and an Acton SP-2758 Imaging Spectrograph and Monochromator (Princeton Instruments). The polarized state and the oblique incidence were measured, respectively. Due to the wavelength limitation of the spectrometers, the spectra are measured separately. From the simulations in Fig. 3, there are no obvious resonant peaks at the range from 1.0 μm to 1.4 μm. The other spectrometer also measured that the detected signal is close to the noise level at this range.

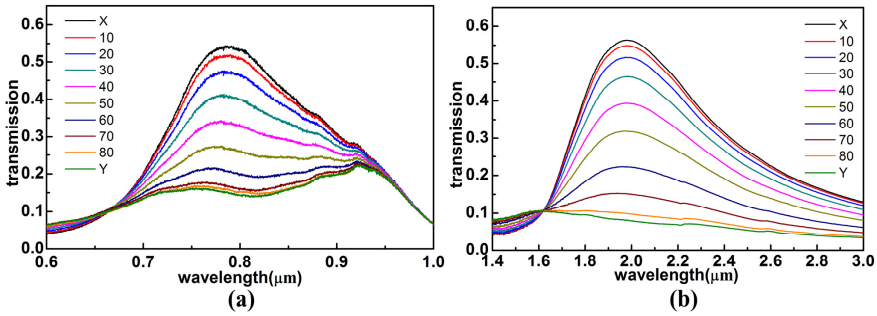

Fig. 6. The experimental results of the structure under different polarization states: (a) the SW peaks and (b) the LW peaks.

The anisotropic transmission was observed in Fig. 6. When the polarization is along the x-axis, the peaks at 0.788 μm and 1.97 μm are in accord with the simulation. According to the discussion above, it is known that the peaks in the SW region are dominated by the small rectangle ('A') lattice and the ones in the LW region are primarily due to the center big rectangle ('B'). Along x-axis, the period of the big hole ('B') array is 0.9 μm while that of the smaller one ('A') is 0.3 μm. When the lattice constant is increased, the peak shifts towards the long wavelength [14]. For y-axis polarization, two bumps at 755 nm and 925 nm are observed while the LW peak seems to be invisible. This is because the LSPs around the apertures greatly influence the transmission when the lattice constant is fixed. As the polarization changes from x- to y-axis, the LSPs are changed. They are also influenced by the tiny distance between the different size holes. Meanwhile, big holes inserted into the small hole array affect the periodic condition, resulting in the SPPs' local concentration. The local coupling between SPPs and LSPs are greatly enhanced, which results in two transmission peaks. For weak intensity in the LW region, the transmission is difficult to measure [5, 14, 17]. It is achieved a polarization-manipulated dual-band transmission in this structure.

From the experiment, it is found that the x-polarized transmission is much more intensive than the y-polarized one. Considering this situation, the transmission as a function of the incident angle in x-axis polarization was measured. As shown in Fig. 7, the positions of the peaks hardly change. This is also in accord with the simulations. According to the discussion above, the coupling between the affected SPPs and the LSPs greatly enhances the local resonance, leading to the angle invariance. At the SW peak, the intensity is reduced by 6% while it is a 45% reduction at the LW one. For the LW peak, its intensity is much more easily affected by the input intensity than the SW one. The incident intensity becomes weaker when

#202368 - $15.00 USD Received 2 Dec 2013; revised 17 Jan 2014; accepted 17 Jan 2014; published 27 Jan 2014

the angle of incidence varies from 0 to 30 degrees. Then the big hole ('B') is changed more in intensity because its area is 8 times bigger than that of the small ('A') one. As a result, the intensity of the right peak declined more than that of the left one. Nevertheless, this structure displays incident angle invariance transmission in a 30-degree range. The high transmission and excellent angle invariance are useful in probing in near-field. When the incident angle is over 30 degrees, the intensity tends to zero.

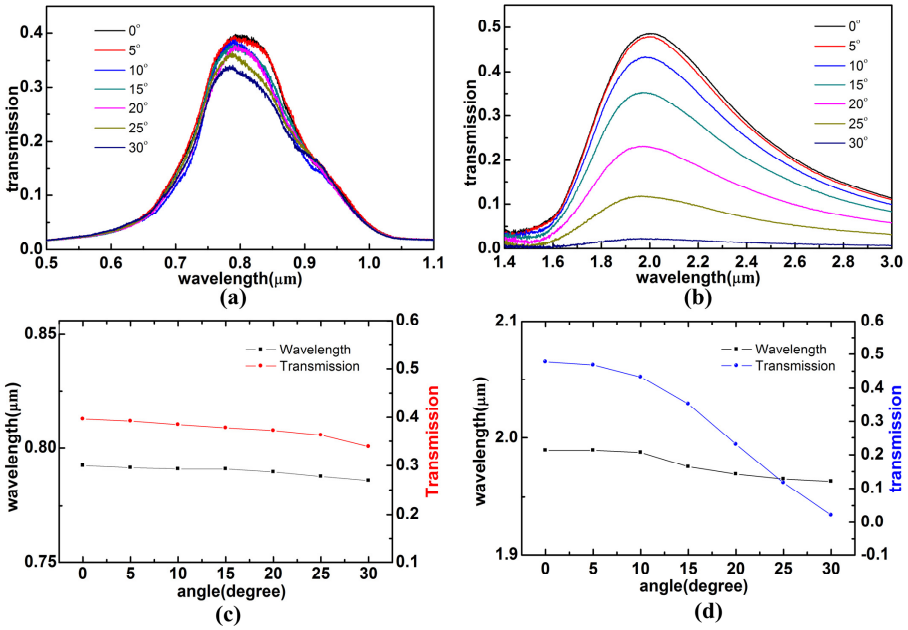

Fig. 7. The transmission spectra of the 0.788 μm peak (a) and the 1.97 μm peak (b) at different incident angles, respectively. Angle invariance and corresponding transmission intensity of the two peaks: the 0.788 μm peak (c) and the 1.97 μm peak (d) for various oblique incidence cases.

Multi-band anisotropic transmission simultaneously can also be achieved. The method is to construct a higher order RSC structure by adding more different sized holes into the array. In general, the experimental results demonstrate that the multi-band anisotropic transmission can be achieved through rectangular Sierpinski-Carpet aperture array, and meantime the structure shows good incident angle invariance which is superior to ordinary rectangle arrays.

4. Conclusion

The rectangular Sierpinski-Carpet aperture array has an unusual property distinct from ordinary rectangle array. Different wavelengths can be simultaneously excited and they are independent on the incident angle in 30 degrees. These findings result from the effects of different sized holes aligned together. For the fractal-featured array, the transmission is not primarily due to the SPP effects but also influenced by LSPs and aperture modes together. Taking advantage of the self-similarity and the high compressibility of the fractal structure, the RSC aperture array provides a proposal to achieve multi-band anisotropic transmission and oblique invariance by squeezing different size holes in finite area. It will have a potential application in integrated light-emitting device, detective device and displays [20].

Acknowledgments

This work was supported from the National Natural Science Foundation of China (Grant 61178014), and the key project of the Ministry of Education of China (Grant 109061).